

Iacopo Bernetti<sup>1</sup>, Lorenzo Bambi<sup>2</sup>, Elena Barbierato<sup>1</sup>, Tommaso Borghini<sup>2</sup>, Irene Capecchi<sup>1</sup>

<sup>1</sup> *Department of Agriculture, Food, Environment and Forestry – DAGRI, Università degli Studi di Firenze, Italy*

<sup>2</sup> *Department of Architecture – DIDA, Università degli Studi di Firenze, Italy*

E-mail: [iacopo.bernetti@unifi.it](mailto:iacopo.bernetti@unifi.it);  
[lorenzo.bambi@unifi.it](mailto:lorenzo.bambi@unifi.it); [elena.barbierato@unifi.it](mailto:elena.barbierato@unifi.it);  
[tommaso.borghini@unifi.it](mailto:tommaso.borghini@unifi.it); [irene.capecchi@unifi.it](mailto:irene.capecchi@unifi.it)

Keywords: *Wind energy, Eye-tracking, Environmental trade-offs*

Parole chiave: *Energia eolica, Eye tracking, Trade-off ambientale*

JEL codes: Q26

## **A decision support system for assessing the perception and acceptance of WTs in high-value landscapes: The case of Chianti Classico (Italy)**

Renewable energies are fundamental to future development. Such technologies reduce air pollution and improve air quality; however, they can generate other types of environmental problems, which must be investigated. The location of structures is one of these problems, which involves visual impacts and is a primary factor affecting public reaction. Our work was concerned with the visual impact and the alterations to the landscape made by wind turbines. The main goal was to establish the factors and attributes of a wind farm that determine the perception and aesthetic preferences of people, with a particular emphasis on representatives of Generation Y. This group was chosen because they represent the most dynamic, innovative, and creative social group. Thus, we proposed some design strategies to reduce the visual impact of wind turbines.

---

### **1. Introduction**

#### *1.1. General Problem*

Innovative technologies are developed to reduce emissions and slow global warming by climate change caused largely by CO<sub>2</sub> emissions from human-related energy production, population growth, and consumption patterns. One of the CO<sub>2</sub> neutral energy generation technologies is wind power production. The wind is a renewable energy source that can be used nearly worldwide and is limited only by atmospheric conditions and the capacity and spatial extent of electricity networks.

#### *1.2. Literature Review*

The visual impact is difficult to assess quantitatively in an objective way. A wind turbine (WT) that can be seen from a location does not itself comprise an adverse impact because visibility is not the same as a sensed visual impact. Leaving aside works that analyzed the visual impact of WT installation locations “a priori” (Ladenburg *et al.*, 2013; Wróżyński *et al.*, 2016), many authors take into account the intervisibility from countries and villages in the territory (Hurtado *et al.*, 2004). Möller (2006) summarized land use or population counts for cumulative numbers of visible WTs. Rather than quantifying absolute exposure, this established a

benchmark for comparison. Georgiou and Skarlatos (2016) calculated the views-hed from primary roads.

Many authors have verified that the sensitivity of people to the placement of WTs in landscapes with high-aesthetic quality is greater (de Vries *et al.*, 2012; Molnarova *et al.*, 2012). For our study, the locations sensitive to the impact of WTs are the cultural landscapes with the highest visual value. Therefore, for the assessment of the visual impact of the energy facilities, an objective method of assessing the aesthetic value of the landscape is required.

The most widely used technique for assessing the visual impact of WTs is the insertion through photomontage in photographic images (see o.a., Betakova *et al.*, 2015; Maehr *et al.*, 2015; Arnberger *et al.*, 2018). Few studies have evaluated the visual impact of an existing or future wind farm infrastructure using virtual reality VR (Ruotolo *et al.*, 2013; Yu *et al.*, 2017). VR offers an excellent opportunity for environmental impact studies (Iachini *et al.*, 2012; Maffei *et al.*, 2013; Ruotolo *et al.*, 2013). VR allows the presentation of a multisensory environment with incorporated auditory and visual components and allows an experience highly similar to that of real life. By allowing people to experience a wind farm environment and explore their perceptions, VR technology can provide unique data with which to optimize the numbers, types, and positions of WTs (Wan *et al.*, 2012). The use of 360° interactive photographs and videos through the VR headset allows interactive and immersive visualization of the space that surrounds the interviewee approximating the real experience in space. Generally, the assessment of the visual impact of WTs is conducted by eliciting a rating from an interviewee (see o.a., Yu *et al.*, 2017). However, the use of evaluations through questionnaires can be biased because of strategic responses caused by prejudices or favorable attitudes (Cass and Walkker, 2009; Warren *et al.*, 2005). In our work, we used the eye-tracking technique combined with VR to conduct an unbiased assessment of the perceptions regarding WTs in the landscape.

Finally, a few authors (Strazzera *et al.*, 2012; Mariel *et al.*, 2015) have attempted to analyze the trade-offs between the two main social benefits, landscape conservation and the reduction of carbon emissions, to provide policy land for the best choice of technical alternative in terms of the number and size of WTs in a wind energy facility installed in a specific territory.

### 1.3. Purpose of the Research

The purpose of our study was to create a prototype of a spatial decision support system that integrates models of visual impact detected with VR and eye-tracking, landscape value models based on data shared on social media, and models of carbon footprints in a GIS environment to identify the technical characteristics of wind energy facilities that represent the best compromise between emission reduction and conservation of the landscape. The spatial decision support system will be tested in an area with a high-landscape value in Tuscany (Italy), the appellation of the Chianti Classico area. This goal of this study was to analyze the per-

ception of the cultural landscape, with a particular emphasis on representatives of Generation Y (so-called millennials, which are a population cohort born between 1980 and 2000), in the context of the development of wind energy identified through the location of wind power plants. In a recent study, Rogatka *et al.* (2017) found that generation Y will be the most sensitive social group both to landscape conservation and to climatic and energy issues.

The decision support system was implemented through the following phases:

- a) Identification of locations with high-landscape value through data shared on social media platforms.
- b) Evaluation of the energy productivity derived from a set of wind farms of different size and power.
- c) Evaluation of the perception and acceptance of WTs through an eye-tracking experiment using landscape simulations administered via VR to a sample of subjects.
- d) Formulation of a multi-objective analysis model for the choice of the best compromise between energy production and perceived landscape impact.

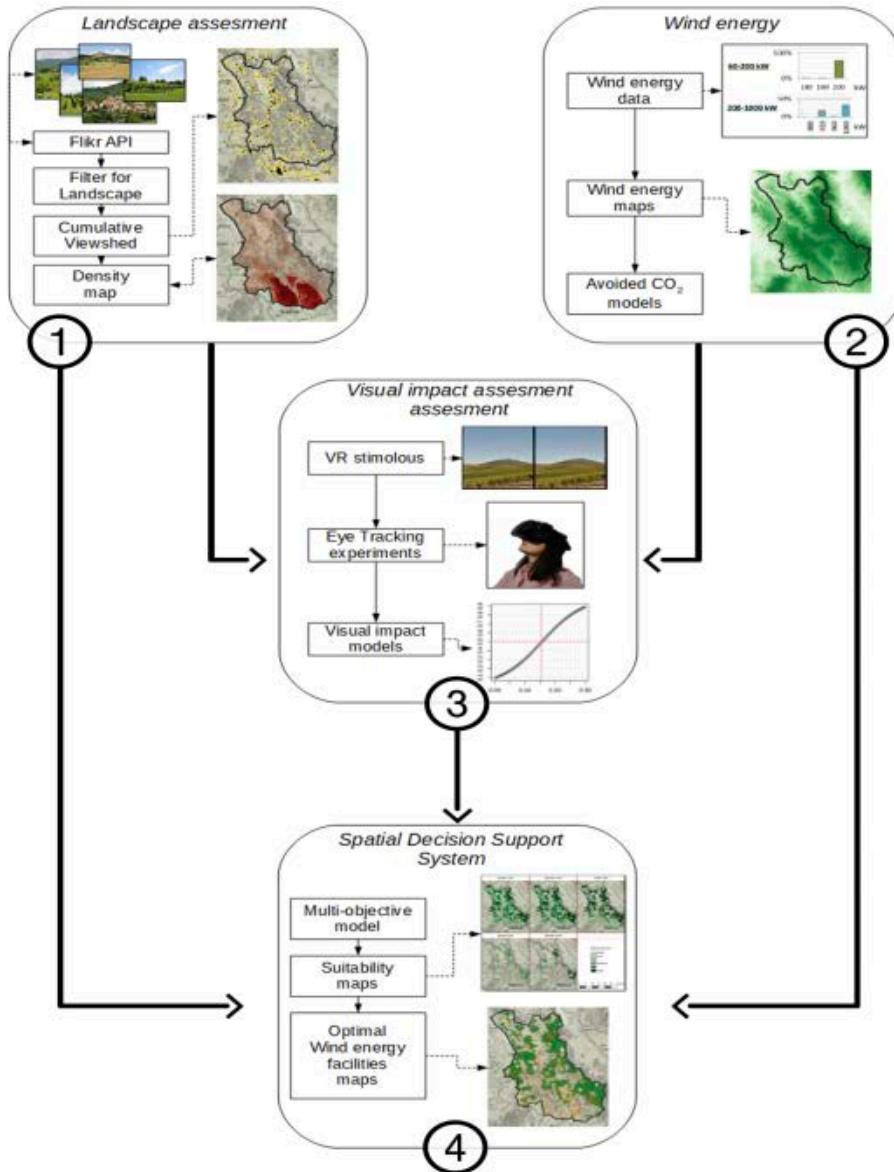
## 2. Methodologies

### 2.1. Landscape Evaluation

For the identification of locations of cultural landscapes with high-visual value, we used the method of spatial density of shared photos on the Flickr social media platform. Wood *et al.* (2013) showed that evidence of actual visitation could be predicted using the density of geotagged Flickr photos. Levin *et al.* (2017, p. 122) found strong and significant correlations between all crowdsourced data and visitation statistics, demonstrating the potential to use crowdsourcing data to characterize the social and perceived importance of protected areas and as a proxy for visitation statistics. The geographical distribution of the geotagged photos can provide useful information for determining the most attractive locations in the territory. In the literature, several methods have been proposed to analyze the geographical concentration of information from social networks. We used a density analysis to outline areas of high-photo concentration. The point data were transformed into a density surface using an analysis of Kernel Density Estimation (KDE) (Chen and Shaw, 2016) with an Epanechnikov kernel with a bandwidth chosen to maximize the point process likelihood cross-validation criterion (Loader, 1999). Kernel density calculates the density of point features around each output raster cell. Conceptually, a smoothly curved surface is fitted over each point. The surface value is highest at the location of the point and diminishes with increasing distance from the point, reaching zero at the search radius distance from the point. Consistent with the geographical scale of the case study, we chose a search radius of 500 m.

As an index of visual sensitivity of points with high-cultural-landscape value, we used the cumulative viewshed method calculated from high-density lo-

Figure 1. The structure of the spatial decision support system.



cations. Visibility analysis is increasingly applied by landscape planners as well, being a useful decision support system because it deals with the best possible spatial arrangement of land uses and assesses the visual impact of given features in the landscape (e.g., Bell, 2001; Bryan, 2003; Hernández *et al.*, 2004; Palmer and Hoffman, 2001). Perhaps the most popular concept used to explore visual space

in a landscape has been the cumulative viewshed (Wheatley, 1995; Ramos and Pastor, 2012), sometimes called total viewshed or intrinsic viewshed (Franch-Pardo *et al.*, 2017). In general, cumulative viewsheds are created by repeatedly calculating the viewshed from various viewpoint locations and then adding them using map algebra to produce a single image. We defined and calculated each viewshed using a digital terrain model (DTM) of 10 m from a height of 165 cm and within a maximum radius of 15 km. We used this value because, in the analyzes carried out in the campaign for the protection of rural Wales (Sullivan *et al.*, 2012), wind structures were considered the main focal points of visual attention from 12 to 19 km.

### 2.2. Energy Production

Wind energy production maps are the most important data for assessing the energy potential of a territory. In our study, we used the maps of wind producibility realized with the WINDGIS project (Mari *et al.*, 2011). In addition to the average wind speed, the WINDGIS geodatabase contains FLHs at heights of 25, 50, 75, and 100 m. A full-load hour is at full-wind capacity. It is the capacity it will take a given WT to yield its annual production if it can produce its installed capacity. For the definition of turbine power to be used in the impact assessment, we referred to the statistical report on energy from renewable sources in Italy (GSE 2018). As shown in Figure 2, the WTs installed in Italy are primarily those with low pow-

Figure 2. Number and capacity of wind power plants installed in Italy. Data are from the Italian company “Gestore Servizi Energetici (GSE).”



Table 1. Technical data on the WTs used in the evaluation models.

Power	Model	Height of pole (m)	Rotor diameter (m)
60 kW	GHRE POWER FD25-60	30/36	25
200 kW	SEI NW 200/29	40/50	29
1000 kW	GHRE POWER GW 93-1000	75/85	93

er (60 kW), medium power (200 kW), and medium-large power (1 MW). Table 1 shows the technical data for the WTs used in the evaluation models.

### 2.3. Wind turbine Perception and Social Evaluation

VR technology is an advanced technology that combines a high degree of control and ecological validity and is capable of simulating experimental conditions reasonably similar to those in a real environment. In our research, we used VR to create stimuli through 360° panoramic photos of the landscape, such that participants could immerse themselves in the virtual world through VR devices, expecting to have the same experiences as in the real landscape. The key to the accuracy of VR technology lies in the realization of the “presence,” which arouses the sensation of physically “being there” through the virtual environment, such that the virtual environment can reproduce the experience of the user in the real environment.

In our study, we inserted the WTs of the different powers investigated by photomontage in the spherical photos simulating a distance from the observer from a minimum of 1.1 to a maximum of 6 km. At this level, WTs visually dominated the space because of their height, which occupies an important amount of space. They are attractive without moving blades. However, at these distances, the acoustic impact is negligible even for the turbines with the greatest power among those considered in this study (Rogers *et al.*, 2006). For these reasons, only the visual impact must be considered, and therefore, this is different from that of previous studies. VR was used without acoustic simulation.

The eye-tracking allows the detection of the direction of the gaze of the individual who observes a landscape. When observing visual scenes, the resulting eye movements are not simply a set of random fixations. Instead, the fixations exhibit a specific pattern according to a specific strategy embedded in the human nervous system (Dupont *et al.*, 2016). When observing images, attention will be allocated only to a limited part of the image. Two main aspects influence how attention is distributed: the content of the scene (bottom-up, low-level process) and the cognitive characteristics of the observer top-down, high-level process (Rajashekar and van der Linde, 2008). The fast bottom-up mechanism is always operating – although stronger in free-viewing situations – the top-down mechanism predominantly comes into effect when performing tasks; for example, answering a ques-

tionnaire (Borji *et al.*, 2013). In the particular case of landscapes, the bottom-up processes will mainly drive the observation because people usually observe scenes freely and without a task in mind (Dupont *et al.*, 2016). Consequently, the distribution of fixations will be primarily guided by the content of the visual stimulus. This technique might be useful in landscape planning, architecture, and design, and in particular, in visual impact assessments of new projects; for example, estimating how well different wind energy facilities are visually integrated into the surrounding landscape. Fixation times aggregated for a type of content, such as WTs, can be used as an indicator of the amount of cognitive processing related to that type of content (Duchowsky, 2007).

The preparation of the stimuli to be evaluated through VR and eye-tracking was divided into the following phases. First, six locations corresponding to high-value cultural landscapes were identified through the map of Flickr photo density. On these points, we downloaded the 360° spherical images from the Google Street View database. These images could be played in VR through a VR headset. The 360° spherical images have a spherical projection covering 360° in the horizontal and nearly 180° degrees in the vertical field of view. For this reason, the size of a WT in image pixels is given by its visual angle defined by the arctangent of the height of the turbine according to the distance from the observer. Thus, for a spherical image with a height of  $H$  pixels and an angle measured in degrees, the apparent height of the turbine measured in pixels was calculated with the following equation (1):

$$VA_{pixel} = \frac{\tan^{-1}\left(\frac{height}{distance}\right)}{180} H \quad (1)$$

Applying this method 12 photomontages of spherical photos were constructed (Table 2). The visual stimulus of the single WT and the wind power facility was created using the Unity 3D software. Each stimulus consisted of a sequence of six photomontages as shown in Table 2.

Eye-tracking was performed running Pupil Labs open source eye-tracking software, which captures pupil dilation. This software works with the Pupil Labs eye-tracking hardware integrated into the HTC Vive head-mounted display (Figure 3).

In the first run, the participants were asked to look at the six landscapes without a task. This bottom-up perception enabled an unbiased exploration of the landscape without directing the attention of the participants to specific elements. At the end of the vision of each 360° image, the participants answered the following questions:

1. In this landscape there are WTs, could you see them? Yes/No.
2. If yes, did they disturb you? Yes/No.

Finally, at the end of the stimulus, this last question was asked:

3. Is landscape protection or renewable energy production more important? Rating scale from 1 = landscape preservation up to 5 = renewable energy.

Table 2. Stimulus data.

Observation point (Goggle Street View location)	WT power	Cluster	Angle of view (degrees)	Stimulus
1	60 kW	1	0.55	2
			2.42	1
2	60 kW	1	0.44	1
			6	2
3	60 kW	6	2.97	2
			4.29	1
4	1 MW	1	1.54	1
			6.49	2
5	1 MW	1	1.21	2
			6	1
6	1 MW	6	8.14	1
			11.66	2

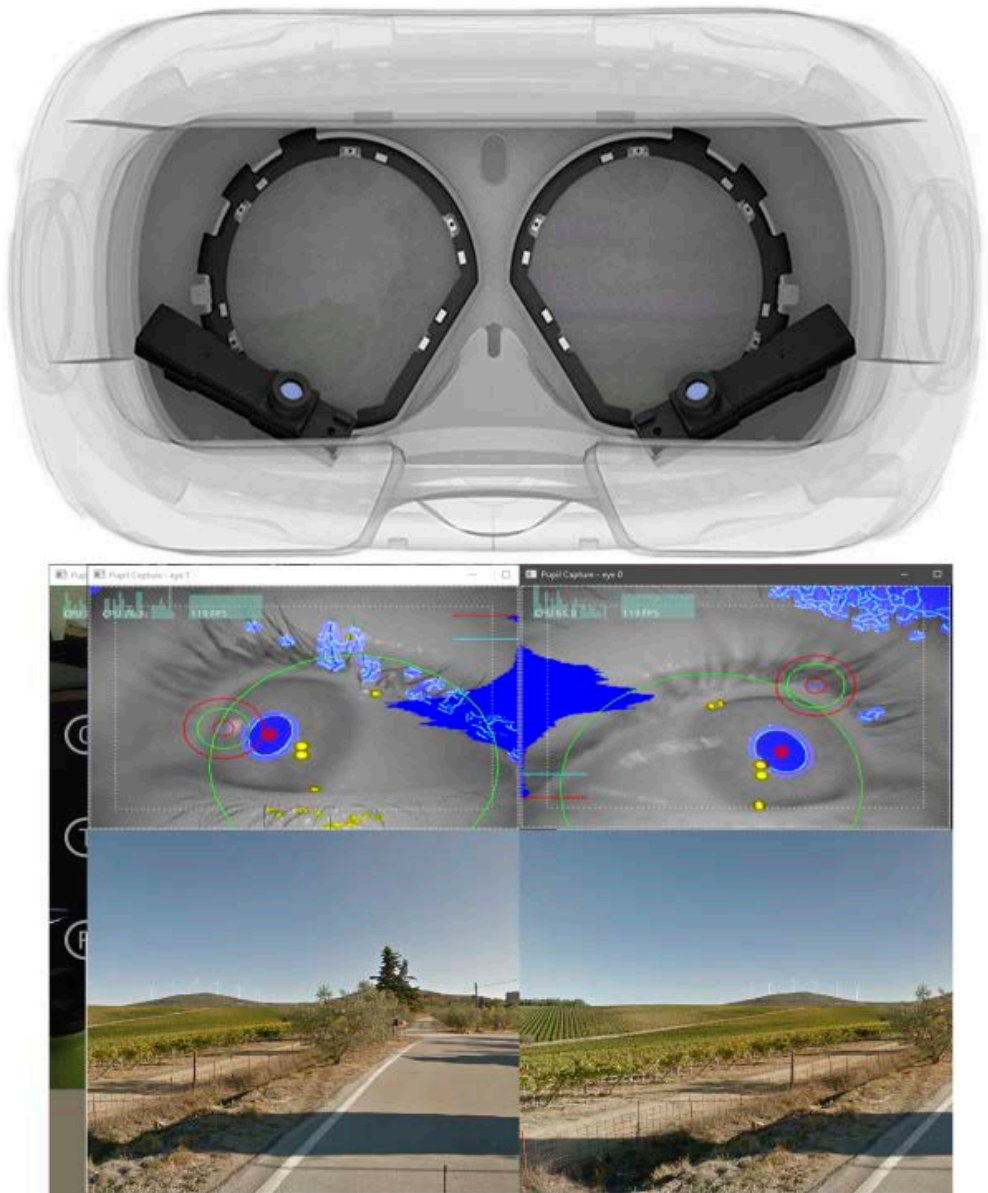
#### 2.4. The trade-off from landscape and wind energy production as a multiple objective decision problem

A conflict between wind energy production and conservation of cultural landscapes occurs if areas of high-visual value are suitable for the production of wind energy. The trade-offs between green energy production and landscape conservation can be analyzed and solved through a multi-objective approach. For each territorial location (pixel of a raster map) it is necessary to identify the energy technical alternative that maximizes the production of territorial energy and minimizes the impact on the landscape. The general form of this problem is shown in the following equation:

$$\begin{aligned}
 & \max_i \{W_{GrEn}GrEn(i, j)\} \\
 & \min_i \{W_{ImpLand}ImpLand(i, j)\} \\
 & \text{s.t.} \\
 & Prob_{i,j}(dist = yes) < 0.5 \\
 & AvCO_2(j, i) > 0
 \end{aligned} \tag{2}$$

where  $i = \{1, 2, \dots, n\}$  territorial location (pixels of a raster map);  $j = \{60kW1WT; 60kW6WTs; 200kW1WT; 200kW6WTs; 1MW1WT; 1MW6WTs\}$  are technical alternatives to wind energy facilities;  $GrEn(i, j)$  is the environmental (positive) impact derived from the use of renewable energy in location  $i$  and for the wind energy facility  $j$ ;  $ImpLand(i, j)$  is the landscape (negative) impact;  $W_{GrEn}$  and  $W_{ImpLand}$  are, respec-

Figure 3. Pupil Labs eye tracker for HTC VIVE.



tively, weights representing the social benefit derived from renewable energy and landscape conservation;  $Prob_{i,j}(\downarrow)$  is the ( $\downarrow$ ) probability that people felt disturbed in location  $i$  when viewing the wind energy facility  $j$ ;  $AvCO_2(i,j)$  are the tons of net  $CO_2$  avoided per year in location  $i$  for the  $j$ -th facility.

As an indicator of the environmental impact of wind energy production using WTs, the amount of net CO<sub>2</sub> avoided was chosen. The net annualized emissions in the life cycle of the WT was calculated according to the method proposed by Smoucha *et al.* (2016). Formally:

$$AvCO_2(i, j) = WindCO_2(i, j) - \frac{LCycCO_2(j)}{lifespan(j)} \quad (3)$$

where  $WindCO_2(j, i)$  it is the annual CO<sub>2</sub> avoided through the production of wind energy using WT  $j$ ;  $LCycCO_2(j)$  is the CO<sub>2</sub> output during the life cycle of the WT;  $lifespan(j)$  is the WT lifespan. The CO<sub>2</sub> avoided the production of wind energy  $WindCO_2(i, j)$  depends from the power of the turbine  $j$ ,  $WTPower(j)$ , from the full-load hours in the location  $i$ ,  $H(i)$  and from the coefficient of the emission of tons of CO<sub>2</sub> emitted per MW of energy produced using fossil fuels  $I$ :

$$WindCO_2(i, j) = WTPower(j) \cdot H(i) \cdot I \quad (4)$$

Considering that the most used fossil energy source for the production of electricity in Tuscany is gas,  $we$  was set as  $I = 0.490$  t/MW. Finally, the index was normalized in the interval  $[0,1]$ :

$$GrEn(i, j) = \frac{AvCO_2(i, j) - \min_i [AvCO_2(i, j)]}{\max_i [AvCO_2(i, j)] - \min_i [AvCO_2(i, j)]} \quad (5)$$

The landscape impact index was derived from two sub-indices, the first was related to the perception of the wind energy plant and the second to the value of the cultural landscape in which the plant was perceived.

The perceptibility index used was the time to the first fixation derived from the eye-tracking experiment. The time to the first fixation indicated the amount of time taken by an interviewee (or all respondents on average) to look at a specific disturbance element from the beginning of the stimulus. Therefore, the time to the first fixation could be a suitable measure to study the disturbance by landscape elements, such as WTs. The time to the first fixation is a basic metric but valuable in eye monitoring and can provide information on how some aspects of a visual scene are prioritized (Noland *et al.*, 2017). The time to the first fixation was therefore considered as inversely proportional to the (negative) impact of the wind energy system. To calculate the time to first fixation (TTFF( $i, j$ )) for each location  $i$  and every alternative  $j$ , we used the following method. We first calculated the non-dimensional visual impact index, NI ( $j$ ) of each wind energy facility  $j$ . NI was defined as the ratio of the two visual angles (see Rodrigues *et al.*, 2010; Minelli *et al.*, 2014):

$$NI(i, j) = \frac{A_{obj}(i, j)}{A_{fov}} \quad (6)$$

where  $A_{fov}$  is the angle of the human vertical field of view (approximately 135°).  $A_{obj}$  is calculated as the perceived angle subtended by WT( $j$ ):

$$A_{obj}(i, j) = \left( \tan^{-1} \left( \frac{E(i) - E(l) + H(j)}{D(i, l)} \right) - \tan^{-1} \left( \frac{E(i) - E(l)}{D(i, l)} \right) \right) \cdot nWT(j) \quad (7)$$

where  $E(i)$  is the elevation of the location  $i$ ;  $E(l)$  is the elevation of the nearest high-landscape-value location  $l$ , as calculated from the map of the density of points of shared photos on Flickr;  $D(i, l)$  is the distance from  $l$  to  $i$ ;  $nWT(j)$  is the number of WTs (1 or 6) in alternative  $j$ . Finally, we calculated the relationship between NI ( $i, j$ ) and TTFF ( $i, j$ ) based on the data collected through the eye-tracking survey using a log-log regression:

$$TTFF(i, j) = a \cdot NI(i, j)^{-b} \quad (8)$$

The second index was calculated through the Flickr points intervisibility map. We constructed a dimensionless indicator [0,1] based on the hypothesis that the locations with the maximum landscape value were those framed by at least 10% of the photo shooting locations shared on Flickr, according to the following report:

$$ImpView(i, j) = \begin{cases} 1 & \text{if } View_{i,j} \geq P_{10\%}(View_{i,j}) \\ \frac{View_{i,j}}{P_{10\%}(View_{i,j})} & \text{if } View_{i,j} < P_{10\%}(View_{i,j}) \end{cases} \quad (9)$$

where  $ImpView(i, j)$  is the impact indicator related to the value of the cultural landscape for location  $i$  and alternative  $j$ ;  $View_{i,j}$  is the cumulative value for viewshed maps;  $P_{10\%}(View_{i,j})$  are the tenth percentiles of the cumulative viewshed maps. Both indicators were normalized in the range [0,1].

Considering that the visual impact on the landscape is an objective to be minimized and that the maximum suitability is obtained with the minimum impact, the normalization procedure was the following:

$$\begin{aligned} NTTF(i, j) &= \frac{TTFF(i, j) - \min_i[TTFF(i, j)]}{\max_i[TTFF(i, j)] - \min_i[TTFF(i, j)]} \\ NImpView(i, j) &= \frac{\max_i[ImpView(i, j)] - ImpView(i, j)}{\max_i[ImpView(i, j)] - \min_i[ImpView(i, j)]} \end{aligned} \quad (10)$$

The aggregate visual impact indicator on the landscape was calculated by the minimum operator:

$$ImpLand(i, j) = \min[NTIFF(i, j), NImpView(i, j)].$$

The last element of the model is the constraint. The probability that a person feels disturbance when viewing a WT  $j$  from the location  $i$  was estimated through

a logistic regression that correlated the (binary) results obtained from question 3 of the questionnaire with the non-dimensional visual impact index, NI (i, j):

$$P_{i,j}(\text{disturb} = 1 | \text{NI}_{i,j}) = \frac{1}{1 + e^{-(a+b \cdot \text{NI}_{i,j})}} \quad (11)$$

The multi-objective model was solved with the weighted linear combination. For each alternative j, a suitability map was calculated using the following:

$$\text{Suit}(j) = \max(W_{GrEn} \cdot GrEn_{i,j} + W_{ImpLand} \cdot ImpLand_{i,j}) \cdot \begin{cases} 1 & \text{if } Prob_{i,j}(\text{dist} = 1) < 0.5 \\ 0 & \text{if } Prob_{i,j}(\text{dist} = 1) \geq 0.5 \end{cases} \quad (12)$$

The weights were calculated in proportion to the answers given to question 2.2 of the questionnaire.

### 3. The study area

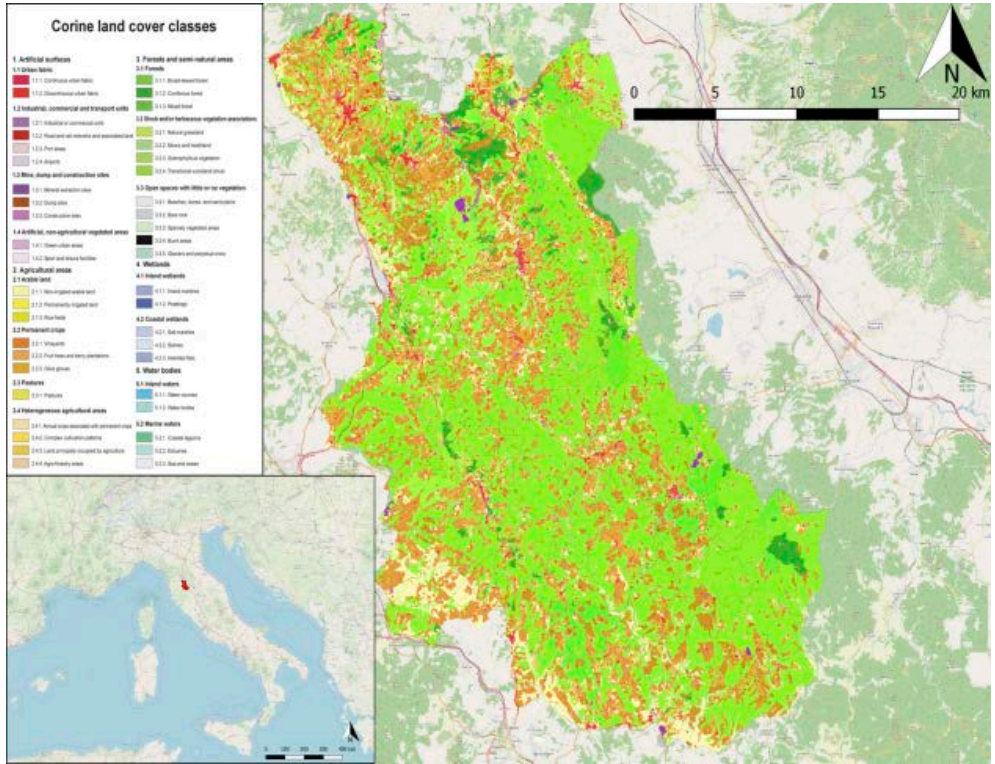
The territory of the Chianti Classico (Figure 4) extends for 71,800 ha located between the provinces of Siena and Florence. The characteristic element of the Chianti agricultural landscape is the rows of vines that alternate with the olive groves. With over 7,200 ha of vineyards registered in the D.O.C.G. register, Chianti Classico is one of the most important appellations in Italy. The enhancement of the territory and landscape of Chianti has its origins since the sixteenth century, when, with the conversion of the Florentine Lordship into the Grand Duchy of Tuscany, banking and commercial activities went into crisis and many investments were directed toward strengthening the primary production. Some forms of production still present today originated from that period (Marone and Menghini 1991). Torquati, Giacché, and Venanzi (2015, p. 122) defined Chianti as a “Traditional Cultural Vineyard Landscape” (TCVL) because the viticulture sector is one of most integrated with the kind of tourism that is interested in quality-food products associated with a specific place of origin. Additionally, the sector, more than others, has responded to market changes by increasing the appeal of their products.

## 4. Results

### 4.1. The landscape evaluation

The geotagged photos were queried from the Flickr API using the statistical software program R using a buffer of 15 km beyond the margin of the study area. The raw database contained approximately 137,000 localizations of photos taken from 2005 to 2017. The pictures containing the tags “agriculture,” “rural landscape,” “vineyard,” “olive,” “grassland,” and related words were filtered. To avoid

Figure 4. Study area.



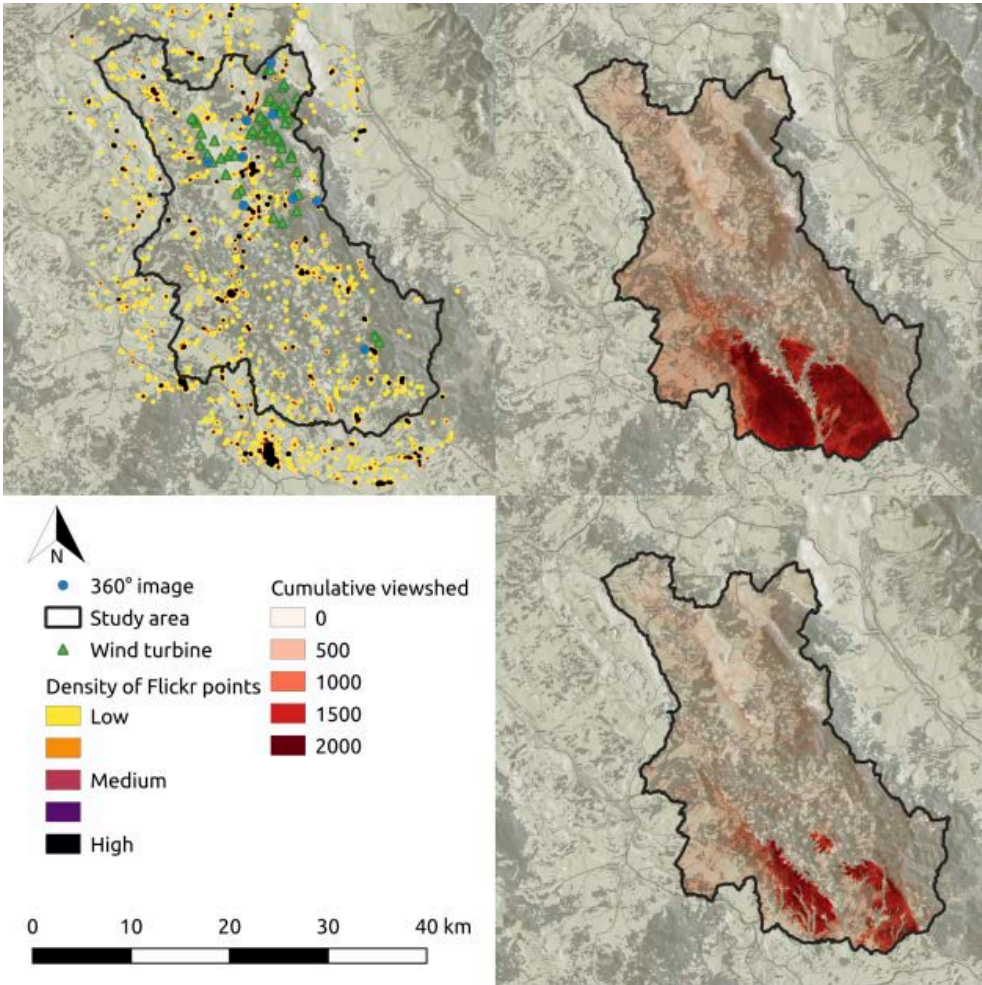
the bias of highly active users, we only included one randomly selected photo per user. The final database contained 4.814 photographic points. Figure 5 shows the density map with the sampling points and the position of the WTs inserted through photomontage in the spherical photos. Additionally, in Figure 5, the maps of the cumulative viewshed for the two sizes of WTs are shown.

The two cumulative viewshed maps show that the most sensitive areas are situated in the southern area near the city of Siena.

4.2. Eye-tracking experiment.

The study involved seven women and eight men, aged between 19 and 39 years (mean = 29), each was submitted to six stimuli for a total of 90 observations. Figure 6 shows the attention heatmap in the landscape scene. Heatmaps are visualizations, which show the general distribution of gaze points. They are typically displayed as a color gradient overlays on the presented image or stimulus. The yellow, orange, red, and violet colors represent in ascending order the number of gaze points that were directed towards parts of the image. In the photos, the position of the WTs is highlighted with a rectangle with blue margins.

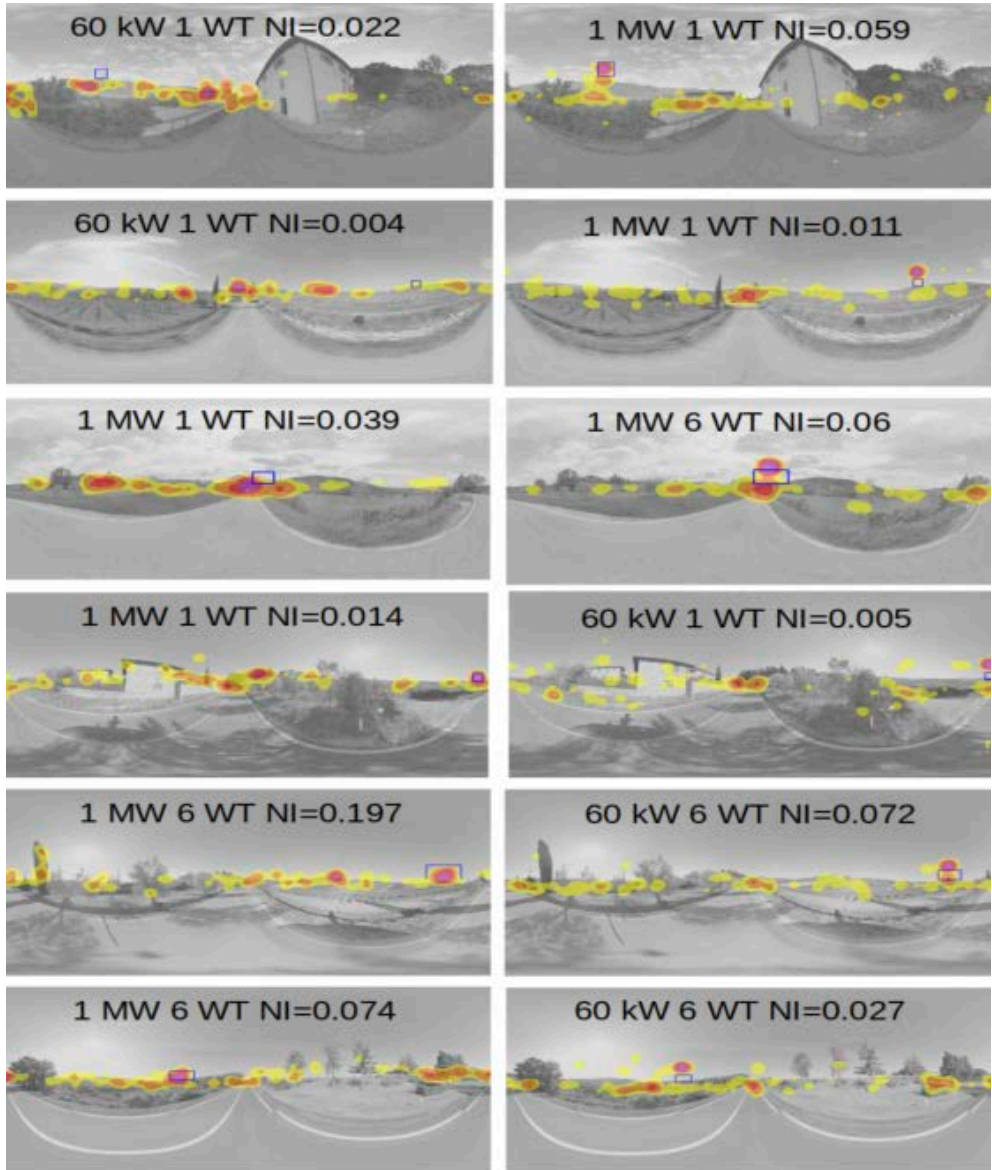
Figure 5. The density map and the map of the cumulative viewshed.



In general, the salient regions in all the photos are those with high contrast, and therefore, high information content, such as buildings in a rural landscape (Dupont *et al.*, 2016) From an evolutionary point of view. These elements can be determined by the Prospectus Theory - Refuge formulated by Appleton (1975). The normal pattern of gaze in most cases is biased by the presence of WTs, especially those with higher visual impact. The most affected heatmaps were those characterized by the presence of wind energy facilities with the highest NI, and thus, confirmed the efficiency of this measure to evaluate the visual impact of WTs.

The portion of the 360° image occupied by the wind energy facility# has been defined as area of interest (AOI) in order to calculate the TTFF metric. An AOI is a tool to select regions of a displayed stimulus and to extract metrics specifically for

Figure 6. Attention heat maps for the landscape scene.



those regions. Through a specific procedure in R language, we calculated the time between the beginning of each experiment and the first fixation on the AOI. Figure 7 shows the boxplots related to time to first fixation frequency distributions. The WT with smaller dimensions registered a much higher time to the first fixation, especially in the case of photos with a single WT. The 60 kW WT had an av-

Table 3. Log-log regression.

	Estimate	Std. Error	t value	Pr(>  t )	
Intercept	1.20784	0.26467	4.564	1.62e-05	***
log(FOV)	-0.33486	0.07116	-4.706	9.34e-06	***

Signif. codes: 0 '\*\*\*' 0.001 '\*\*' 0.01 '\*' 0.05 '.' 0.1 ' ' 1

Residual standard error: 0.8061 on 88 degrees of freedom

Adjusted R-squared: 0.292

F-statistic: 22.14 on 1 and 88 DF, p-value: 9.343e-06

erage time to the first fixation of 17 s for the facility with a single WT and 12 s for the cluster of six WTs against approximately 5 s for both the two 1 MW wind farm facilities.

Table 3 shows the results of the log-log regression between time to first fixation and NI, which will be used in the spatial evaluation model of territorial suitability for wind energy production.

Despite the low correlation coefficient caused by the variability of the participants in the observation of virtual space (Rodeghero *et al.*, 2014), the coefficients were highly significant and it was, therefore, possible to apply the results to the multi-objective model.

By analyzing the answer to question 3 of the questionnaire, it was possible to calculate the weights for the multi-objective model. Figure 8 shows the frequency distribution of the assessment of the importance of renewable energy production in comparison with landscape protection. As reported in the literature, Generation Y is sensitive to the production of green energy (Rogatka *et al.*, 2017).

Normalizing the evaluation, we have  $W_{GrEn}=0.71$  and  $W_{ImpLand}=0.29$ .

Figure 7. Frequency distribution of time to the first fixation.

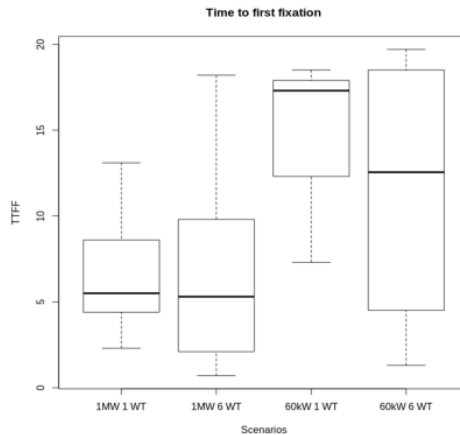


Figure 8. Rating renewable energy vs. landscape conservation.

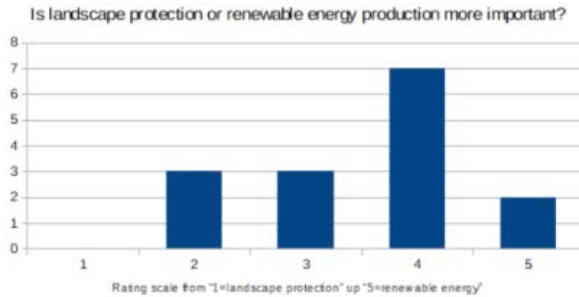


Figure 9. Logit model.

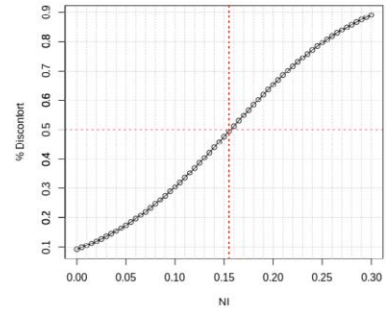


Table 4. Logit model.

	Estimate	Std. Error	z value	Pr(>  z )
Intercept	-2.2792	0.4244	-5.370	7.88e-08
FOV	14.5521	4.3168	3.371	0.000749

AIC: 84.384

The last parameter for the formulation of the multi-objective model was derived from the results of question 2 of the questionnaire. The dependence between NI and the probability that a person felt discomfort upon seeing a WT was examined through a logit model estimated using the maximum likelihood. The model was highly significant (Table 4) and the NI coefficient was positive and significant. The value corresponding to the 50% probability of NI = 0.155 (Figure 9).

#### 4.3. The multiple objective model

The condition  $NI > 0.155$  represents the constraint of the multi-objective model. Using the equations (6) and (7), in the study area, the four maps of the NI visual impact index related to the four wind energy facilities used to realize the stimuli of eye-tracking experiments were calculated. Table 5 shows the quartiles of the frequency distribution of the value of NI. The most influential facility was the cluster of six WTs with 1 MW of power (1 MW 6 WT), whose impact appeared to be incompatible with the landscape characteristics of the Chianti territory. For this reason, this energy facility was not included in the model. To give the model more flexibility, two new technical alternatives based on the 200 kW WT, shown in Table 1, were included. This allowed us to evaluate the transferability of the eye-tracking survey results to different energy plant alternatives. The five wind energy facilities analyzed in the model were: single WT with 60 kW, 200 kW and 1 MW; cluster of six WTs with 60 kW and 200 kW power.

Table 5. Frequency distribution of NI value in maps.

	60 kW 1 WT	60 kW 6 WT	1 MW 1 WT	1 MW 6 WT
Minimum	0.008	0.047	0.022	0.132
First quartile	0.011	0.067	0.031	0.189
Median	0.027	0.164	0.077	0.460
Third quartile	0.046	0.277	0.128	0.771
Maximum	0.094	0.566	0.254	1.525

Table 6. Trade-off of avoided CO<sub>2</sub> vs. landscape conservation.

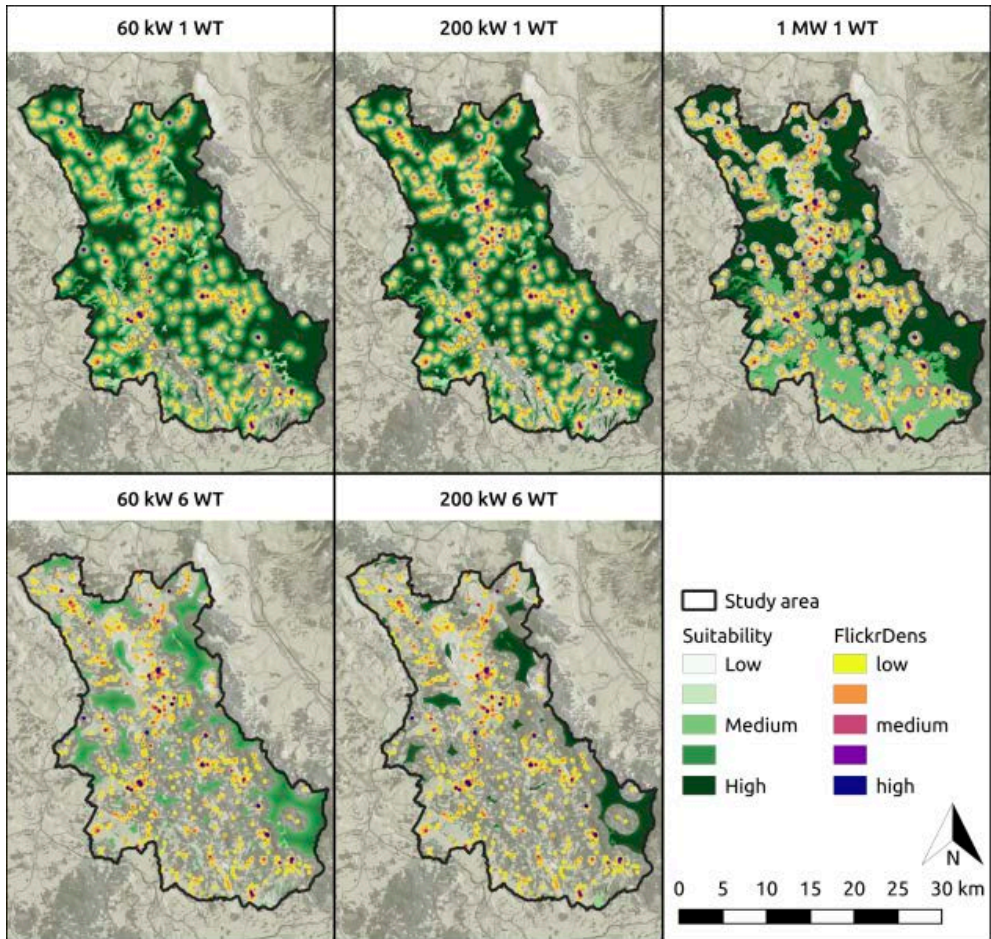
		Minimum	First quartile	Median	Third quartile	Maximum
Avoided CO <sub>2</sub> (t/WT/year)	60 kW 1 WT	-31.55	28.96	30.06	31.30	62.97
	60 kW 6 WT	-189.32	173.75	180.36	187.79	377.80
	200 kW 1 WT	-102.18	99.53	103.20	107.33	212.89
	200 kW 6 WT	-613.06	597.15	619.20	643.98	1277.34
	1 MW 1 WT	431.07	749.65	765.36	783.11	929.45
Landscape index (a dimensional index)	60 kW 1 WT	0.00	0.30	0.47	0.60	1.00
	60 kW 6 WT	0.00	0.13	0.22	0.29	0.51
	200 kW 1 WT	0.00	0.27	0.42	0.54	0.92
	200 kW 6 WT	0.00	0.10	0.19	0.25	0.45
	1 MW 1 WT	0.00	0.04	0.25	0.37	0.69

Table 6 shows, through frequency distributions, the trade-off between landscape conservation index and avoided CO<sub>2</sub> emissions. The WTs of lower power (60 and 200 kW) had a negative carbon balance in unfavorable locations, but in the first quartile, the budgets were all in surplus. Analyzing the characteristic parameters of the CO<sub>2</sub> frequency distribution avoided per year, the most efficient technical alternative was the 1 MW WT. The landscape conservation index instead confirmed a lower impact of the 60 kW WT. It was also interesting to note that for the WTs with a higher power, the 1 MW WT dominated (according to the Pareto rule) the 200 kW WT in the cluster of six WTs.

The suitability maps (Figure 10) show that the constraint of visual impacts strongly reduced the territorial suitability for the production of wind energy in the Chianti area, especially for the energy facilities characterized by a cluster of six WTs.

In the areas furthest away from locations with high-landscape value (areas

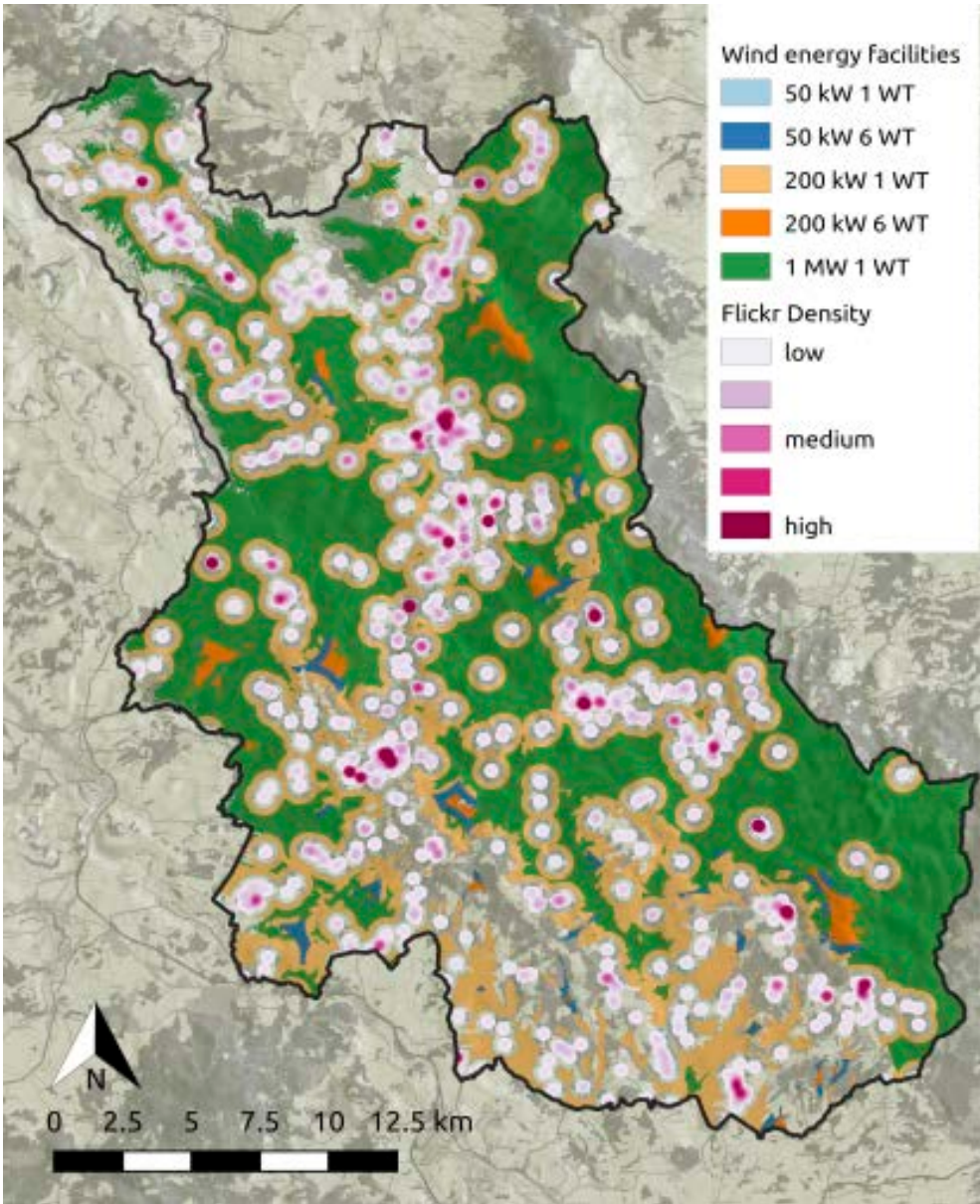
Figure 10. Suitability maps.



with a high density of shooting points of photos shared on Flickr), the wind energy facility that allowed a greater avoidance of the emission of CO<sub>2</sub> (1 MW 1 WT and 200 kW 6 WT) was the most suitable. Instead, the 60 kW WT, especially in the cluster configuration with six WTs, appeared to be the worst alternatives because they had a visual impact slightly lower than the 200 kW equipment; however, poor efficiency in CO<sub>2</sub> balance. These evaluations are summarized in Figure 11, which shows the most efficient technical alternative for each territorial location.

The two most efficient solutions in the study area were the 1 MW single WT in the most distant areas from locations with a high-weight value and the single 200 kW windpipe for the areas that were most sensitive to visual impact.

Figure 11. Optimal wind energy facilities maps.



### 5. Discussion and conclusions

Our study combined wind maps, visual perception models estimated by eye-tracking experiments, and the evaluation of the value of the landscape through

the density of geotagged photos shared on Flickr in a multi-objective model. With this model, we analyzed the trade-offs between visual impacts on the landscape and CO<sub>2</sub> emissions avoided with the production of renewable energy and identified the most efficient wind energy facilities. The results obtained showed that in an area with typical- and high-value landscapes, single WTs with medium power and distant from the most sensitive places were more efficient. However, small turbines were not efficient, even in locations closer to sensitive landscapes.

The results confirmed the findings of recent studies by other research groups who used eye-tracking for landscape impact analysis (Wissen Hayek *et al.*, 2019). The perception time of WTs was significantly influenced by the perceived size of the energy installation. Installations close to the observer and/or with large turbines and/or forming wind farms with many turbines were perceived quickly and the enjoyment of the landscape was felt to be disturbing. The distance factor in the perceived visual impact of the WTs has been studied by many authors, who have obtained different results (Mauro, 2019). Bishop (2002) stressed how, even in clear air, the visual impact of WTs (50 m height; 3-blade rotor; blade 26 m long) “becomes minimal beyond 5–7 km.” The guidelines of the Scottish Natural Heritage (University of Newcastle, 2002), on the other hand, propose three specific distances for the recommended ‘zone of visual influence.’ It suggests a landscape dominated by WTs in the first kilometer of distance (the “immediate area”). The view is mainly occupied by WTs and by the attractive motion of their blades in the “intermediate area” (between 1 and 10 km). On the other hand, the WT visual impact becomes minimal only after 10 km (the “distant area”). Instead, Knies and Gräfe (2011) suggested threshold values quite lower. Similar to that of the Scottish Natural Heritage, they detected several zones of visual impact (proximity, foreground, middle distance, distant view, and far distance) for WTs with different heights (80 m, 100 m, and 150 m), but the proposed visual thresholds were very close to the WT for the “distant view” zone (1.5 km, 2 km, and 2.8 km, respectively), whereas the upper limit of the “far view” zone was between 30 km and 40 km. Values so different depend on the experimental conditions, but above all on the different dimensions of the WTs and the number of elements inside a wind farm. The method proposed in this paper has the advantage of considering these factors. For example, in a work that analyzed three wind energy facilities with 274, 79, and 74 WTs with a tip height of approximately 120 m, Sullivan *et al.* (2012) found that under favorable viewing conditions, the facilities would be unlikely to be missed by casual observers at up to 32 km and that the facilities could be major sources of visual contrast up to 16 km. Although the wind farms analyzed by these authors are very different in size from those considered in this work, applying the logit model of Table 4, we obtain the distance at which the wind facilities disturb at least 50% of the observers is approximately 30 km for the two wind facilities consisting of approximately 70 WTs.

In conclusion, the main result of the study was the realization of a prototype of a spatial decision support system that could be useful for solving the conflict between wind energy production and the conservation of cultural landscapes. The kernel of the spatial decision support system were two models of visual perception of turbines based on surveys using VR and eye-tracking. Another innova-

tive feature of this work was the use of photographs shared on social media to identify the most sensitive landscapes.

Although the proposed method has provided encouraging results, many further developments will be needed. The two models that are the kernel of the present spatial decision support system (Table 3 and 4) will have to be estimated by multivariate analysis taking into consideration many factors critical for visual impact: landscape characteristics, and number of WTs in energy facilities, among others. Besides Generation Y, the sample will have to be extended to other generational groups, from Baby-boomers up to Generation z. The sample of points in which to conduct the simulations must be extended to include urban and natural landscapes among the study areas. Finally, the relationships between WTs and landscape elements (roads, ridges, and field edges, among others) will have to be analyzed. With these further investigations, it will be possible to provide useful indications for minimizing the impact of WTs and also verify the principles of wind-farm design (Heritage, 2009).

## References

- Aly, M., & Bouguet, J. Y. (2012). Street view goes indoors: automatic pose estimation from uncalibrated unordered spherical panoramas. In 2012 IEEE Workshop on the Applications of Computer Vision (WACV) (pp. 1–8). IEEE.
- Appleton, J. (1996). The experience of landscape (pp. 66–7). Chichester: Wiley.
- Arnberger, A., Eder, R., Alex, B., Preisel, H., Ebenberger, M., & Husslein, M. (2018). Trade-offs between wind energy, recreational, and bark-beetle impacts on visual preferences of national park visitors. *Land Use Policy*, 76, 166–177.
- Bell, S. (2001). Landscape pattern, perception and visualisation in the visual management of forests. *Landscape and Urban Planning*, 54(1-4), 201–211.
- Betakova, V., Vojar, J., & Sklenicka, P. (2015). WTs location: How many and how far?. *Applied Energy*, 151, 23–31.
- Bishop, I. D. (2002). Determination of thresholds of visual impact: the case of wind turbines. *Environment and Planning B: Planning and Design*, 29(5), 707–718.
- Borji, A., Sihite, D. N., & Itti, L. (2013). What stands out in a scene? A study of human explicit saliency judgment. *Vision Research*, 91, 62–77.
- Borys, M., & Plechawska-Wójcik, M. (2017). Eye-tracking metrics in perception and visual attention research. *European Journal of Medical Technologies*, 3, 11–23.
- Bryan, B. A. (2003). Physical environmental modeling, visualization and query for supporting landscape planning decisions. *Landscape and Urban Planning*, 65(4), 237–259.
- Cass, N., & Walker, G. (2009). Emotion and rationality: The characterisation and evaluation of opposition to renewable energy projects. *Emotion, Space and Society*, 2(1), 62–69.
- Chen, J., & Shaw, S. L. (2016). Representing the spatial extent of places based on flickr photos with a representativeness-weighted kernel density estimation. In The Annual International Conference on Geographic Information Science (pp. 130–144). Cham, Springer.
- de Vries, S., de Groot, M., & Boers, J. (2012). Eyesores in sight: Quantifying the impact of man-made elements on the scenic beauty of Dutch landscapes. *Landscape and Urban Planning*, 105(1-2), 118–127.
- Duchowski, A. T. (2007). Eye tracking methodology. *Theory and practice*, 328(614), 2-3.
- Dupont, L., Ooms, K., Antrop, M., & Van Eetvelde, V. (2016). Comparing saliency maps and eye-tracking focus maps: The potential use in visual impact assessment based on landscape photographs. *Landscape and Urban Planning*, 148, 17–26.

- Franch-Pardo, I., Cancar-Pomar, L., & Napoletano, B. M. (2017). Visibility analysis and landscape evaluation in Martín river cultural park (Aragon, Spain) integrating biophysical and visual units. *Journal of Maps*, 13(2), 415–424.
- Georgiou, A. G., & Skarlatos, D. (2016). Optimal site selection for siting a solar park using multi-criteria decision analysis and geographical information systems. *Geoscientific Instrumentation, Methods and Data Systems*, 5, 321–332.
- Heritage, S. N. (2002). Visual assessment of windfarms: best practice. University of Newcastle.
- Heritage, S. N. (2009). Siting and Designing windfarms in the landscape. Version 1 December.
- Hernández, J., García, L., & Ayuga, F. (2004). Assessment of the visual impact made on the landscape by new buildings: a methodology for site selection. *Landscape and Urban Planning*, 68(1), 15–28.
- Hurtado, J. P., Fernández, J., Parrondo, J. L., & Blanco, E. (2004). Spanish method of visual impact evaluation in wind farms. *Renewable and Sustainable Energy Reviews*, 8(5), 483–491.
- Iachini, T., Maffei, L., Ruotolo, F., Senese, V. P., Ruggiero, G., Masullo, M., & Alekseeva, N. (2012). Multisensory assessment of acoustic comfort aboard metros: a virtual reality study. *Applied Cognitive Psychology*, 26(5), 757–767.
- Knies, A., & Gräfe, J. (2011). Visibility analysis as a tool for regional planning in the context of “repowering” (wind-turbine upgrading). A transferable example for “North Sea Sustainable Energy Planning, 1–10. Institute for Applied Photogrammetry and Geoinformatics, Oldenburg (Germany)
- Ladenburg, J., Termansen, M., & Hasler, B. (2013). Assessing acceptability of two onshore wind power development schemes: A test of viewshed effects and the cumulative effects of wind turbines. *Energy*, 54, 45–54.
- Loader, C. (1999) Local Regression and Likelihood. New York, Springer.
- Maehr, A. M., Watts, G. R., Hanratty, J., & Talmi, D. (2015). Emotional response to images of wind turbines: A psychophysiological study of their visual impact on the landscape. *Landscape and Urban Planning*, 142, 71–79.
- Maffei, L., Iachini, T., Masullo, M., Aletta, F., Sorrentino, F., Senese, V., & Ruotolo, F. (2013). The effects of vision-related aspects on noise perception of wind turbines in quiet areas. *International Journal of Environmental Research and Public Health*, 10(5), 1681–1697.
- Mari, R., Bottai, L., Busillo, C., Calatrini, F., Gozzini, B., & Gualtieri, G. (2011). A GIS-based interactive web decision support system for planning wind farms in Tuscany (Italy). *Renewable Energy*, 36(2), 754–763.
- Mariel, P., Meyerhoff, J., & Hess, S. (2015). Heterogeneous preferences toward landscape externalities of wind turbines—combining choices and attitudes in a hybrid model. *Renewable and Sustainable Energy Reviews*, 41, 647–657.
- Marone, E., & Menghini, S. (1991). Sviluppo sostenibile: il caso di Greve in Chianti e del Chianti Classico. In 1991 *Atti del XXI Incontro di Studio CESET*, 343–355.
- Mauro, G. (2019). The new “windscares” in the time of energy transition: A comparison of ten European countries. *Applied Geography*, 109, 102041.
- Minelli, A., Marchesini, I., Taylor, F. E., De Rosa, P., Casagrande, L., & Cenci, M. (2014). An open source GIS tool to quantify the visual impact of wind turbines and photovoltaic panels. *Environmental Impact Assessment Review*, 49, 70–78.
- Möller, B. (2006). Changing wind-power landscapes: regional assessment of visual impact on land use and population in Northern Jutland, Denmark. *Applied Energy*, 83(5), 477–494.
- Molnarova, K., Sklenicka, P., Stiborek, J., Svobodova, K., Salek, M., & Brabec, E. (2012). Visual preferences for wind turbines: Location, numbers and respondent characteristics. *Applied Energy*, 92, 269–278.
- Noland, R. B., Weiner, M. D., Gao, D., Cook, M. P., & Nelessen, A. (2017). Eye-tracking technology, visual preference surveys, and urban design: preliminary evidence of an effective methodology. *Journal of Urbanism: International Research on Placemaking and Urban Sustainability*, 10(1), 98–110.
- Palmer, J. F., & Hoffman, R. E. (2001). Rating reliability and representation validity in scenic landscape assessments. *Landscape and Urban Planning*, 54(1–4), 149–161.

- Rajashekar, U., Van Der Linde, I., Bovik, A. C., & Cormack, L. K. (2008). GAFFE: A gaze-attentive fixation finding engine. *IEEE Transactions on Image Processing*, 17(4), 564–573.
- Ramos, B. M., & Pastor, I. O. (2012). Mapping the visual landscape quality in Europe using physical attributes. *Journal of Maps*, 8(1), 56–61.
- Rodeghero, P., McMillan, C., McBurney, P. W., Bosch, N., & D’Mello, S. (2014). Improving automated source code summarization via an eye-tracking study of programmers. In Proceedings of the 36th international conference on Software engineering (pp. 390–401).
- Rodrigues, M., Montañés, C., & Fueyo, N. (2010). A method for the assessment of the visual impact caused by the large-scale deployment of renewable-energy facilities. *Environmental Impact Assessment Review*, 30(4), 240–246.
- Rogatka, K., Chodkowska-Miszczuk, J., Biegańska, J., Grzelak-Kostulska, E., & Środa-Murawska, S. (2017). Perception of the Cultural Landscape Related to Wind Parks—Generation Y Perspective.
- Rogers, A. L., Manwell, J. F., & Wright, S. (2006). Wind turbine acoustic noise. Renewable Energy Research Laboratory, Amherst: University of Massachusetts.
- Ruotolo, F., Maffei, L., Di Gabriele, M., Iachini, T., Masullo, M., Ruggiero, G., & Senese, V. P. (2013). Immersive virtual reality and environmental noise assessment: An innovative audio-visual approach. *Environmental Impact Assessment Review*, 41, 10–20.
- Ruotolo, F., Senese, V. P., Ruggiero, G., Maffei, L., Masullo, M., & Iachini, T. (2012). Individual reactions to a multisensory immersive virtual environment: the impact of a wind farm on individuals. *Cognitive Processing*, 13(1), 319–323.
- Smoucha, E. A., Fitzpatrick, K., Buckingham, S., & Knox, O. G. (2016). Life cycle analysis of the embodied carbon emissions from 14 wind turbines with rated powers between 50Kw and 3.4 Mw. *Journal of Fundamentals of Renewable Energy and Applications*, 6(4).
- Strazzera, E., Mura, M., & Contu, D. (2012). Combining choice experiments with psychometric scales to assess the social acceptability of wind energy projects: A latent class approach. *Energy Policy*, 48, 334–347.
- Sullivan, R. G., Kirchler, L., Lahti, T., Roché, S., Beckman, K., Cantwell, B., & Richmond, P. (2012, May). Wind turbine visibility and visual impact threshold distances in western landscapes. In National Association of Environmental Professionals 37th Annual Conference, May (pp. 21–24).
- Torquati, B., Giacchè, G., & Venanzi, S. (2015). Economic analysis of the traditional cultural vineyard landscapes in Italy. *Journal of Rural Studies*, 39, 122–132.
- Wan, C., Wang, J., Yang, G., Gu, H., & Zhang, X. (2012). Wind farm micro-siting by Gaussian particle swarm optimization with local search strategy. *Renewable Energy*, 48, 276–286.
- Warren, C. R., Lumsden, C., O’Dowd, S., & Birnie, R. V. (2005). ‘Green on green’: public perceptions of wind power in Scotland and Ireland. *Journal of Environmental Planning and Management*, 48(6), 853–875.
- Wheatley, D. (1995). Cumulative viewshed analysis: a GIS-based method for investigating inter-visibility, and its archaeological application. *Archaeology and Geographical Information Systems: a European Perspective*, 171–185.
- Wilmer, E. L., Levin, D. A., & Peres, Y. (2009). Markov chains and mixing times. American Mathematical Soc., Providence.
- Wissen Hayek, U., Müller, K., Göbel, F., Kiefer, P., Spielhofer, R., & Grêt-Regamey, A. (2019). 3D Point Clouds and Eye Tracking for Investigating the Perception and Acceptance of Power Lines in Different Landscapes. *Multimodal Technologies and Interaction*, 3(2), 40.
- Wood, S. A., Guerry, A. D., Silver, J. M., & Lacayo, M. (2013). Using social media to quantify nature-based tourism and recreation. *Scientific Reports*, 3, 2976.
- Wróżyński, R., Sojka, M., & Pyszny, K. (2016). The application of GIS and 3D graphic software to visual impact assessment of wind turbines. *Renewable Energy*, 96, 625–635.
- Yu, T., Behm, H., Bill, R., & Kang, J. (2017). Audio-visual perception of new wind parks. *Landscape and Urban Planning*, 165, 1–10.